Setting the Loading Level of a Wind Power Plant in Power System Planning Stability Studies

Mikhail Y. Borodulin
System and Resource Planning
New York Independent System Operator (NYISO)
Rensselaer, New York, USA
mborodulin@nyiso.com

Abstract-- **In a planning stability study focusing on a specific wind power plant (WPP), it is dispatched at full output. Its dynamic response is not expected to be noticeably affected by the loading of WPPs in close electrical proximity. To investigate the validity of this approach and better understand the mutual effect of the loading levels of nearby WPPs on their dynamic responses to power system faults, four case studies with different local areas and wind turbine generator (WTG) devices are performed. Fault simulations are carried out on real large power system databases. While most numerical experiments confirm the approach, some others suggest that it does not necessarily lead to the severest stability conditions. Further EMTP-type analysis is needed. Meanwhile, and especially when a planning study identifies concerns about the stability of a WPP and/or its fault ride through capability, more combinations of WPP loading levels should be evaluated.**

Index Terms-- **Power system stability, wind turbine generator, wind power plant, dynamic response, fault ride through.**

I. Introduction

Wind energy has become one of the fastest advancing alternative energy technologies. In power system planning studies, stability evaluations for a new wind power plant (WPP) are based on time-domain contingency simulations. Their scenarios mostly involve short circuit faults differing in location, type and clearing procedure. To carry out the simulations, positive-sequence commercial software programs are applied, along with simplified wind turbine generator (WTG) dynamic (stability) models intended for transient stability studies. Essential information about the development and validation of such WTG models can be found in [1]-[3].

Given the multitude of factors affecting the dynamic response of a WPP and, on the other hand, the fact that planning study conclusions are to be made based on a limited number of simulations, the role of study methodology is crucial. In particular, contingency simulations need to be run on a representative set of power flow cases reflecting different load conditions and generation dispatch scenarios. Most often, seasonal high and low load conditions, normal or stressed, are assumed for the power system.

When a planning stability study focuses on a specific WPP, it is dispatched at full output, which is widely thought to be most limiting in terms of its stability performance. When another WPP is very close electrically and, especially, when it shares the same point of interconnection (POI), a potential for mutual dynamic effects should be evaluated. As an example, the investigation of control interaction between multiple WPPs in close electrical proximity [4] shows that their voltage regulators need to be coordinated. However, the dynamic response of a WPP is usually not expected to be noticeably affected by the loading of nearby WPPs. Therefore, their loading is usually defined by the logic of the overall power system dispatch, desired interface flow levels, etc.

Simulation experience, however, has provided evidence that this approach does not necessarily lead to the severest stability conditions, which became an impetus for this work. In particular, the assumption of full output does not necessarily ensure the worst-case stability performance of a WPP and, therefore, more operating conditions should be simulated to adequately assess the fault ride through (FRT) capability of a WPP [5], [6]. The described approach to setting nearby WPPs' loading levels also needs more justification.

This paper discusses setting the loading level of a WPP and the mutual effect of nearby WPPs' loading levels on their dynamic responses to close-in faults. The investigation is based on four case studies with real different local areas and WTG devices. Fault simulations with the Siemens PTI PSS/E software program are carried out on real large power system databases developed by the New York Independent System Operator (NYISO). Since WTG models intended for stability studies are known to be able to exhibit questionable behavior [7], [8], the paper considers model features essential in terms of simulation of partially loaded WTGs.

The work is part of NYISO activities intended to ensure the high quality of wind generation interconnection studies.

II. Study Methodology

At the core, the investigation is based on a large number of numerical experiments on a representative set of network cases with real WPP projects utilizing different WTG devices.

978-1-4673-8040-9/15/$31.00 ©2015 IEEE

A. Local Area

Here, a "local area" of the power system is defined as its relatively small subsystem that includes three nearby WPPs (WPP-1, WPP-2 and WPP-3) whose mutual effect is evaluated. A schematic diagram of a local area is shown in Fig. 1. This topology is only an example; note that the transmission lines directly connecting WPP-2 to the two other WPPs are present only in case study CS#1.

In terms of size, a local area includes system elements no more than several buses away from each of the POIs (assuming the shortest paths, accounting for transmission lines and two-winding transformers but not accounting for zero-impedance branches representing circuit breakers). Most WPPs under consideration in this study seem to be electrically farther from each other than those in [4]. Reactive power devices in the local area, including switched shunts, are modeled "as-is." While their settings can affect transients, analysis of this effect is beyond the scope of the work.

B. Nearby WPPs

For most of the considered WPPs, the active power rating (capacity) P_r is in the range of tens of megawatts (but P_r<150 MW). All short circuit ratio values are above 5. Each WPP-j (j = 1, 2, 3) consists of identical WTGs. The main collector transformers have nominal voltage of either 34.5/115 kV or 34.5/230 kV. None of the WPPs has a plant-level reactive power source (like a STATCOM).

In Fig. 1, each WPP is shown as a single equivalent WTG. However, in most simulations a WPP is represented by a number of equivalent WTGs corresponding to the clusters of the real collector (as it is modeled in NYISO databases).

C. WTG Devices and Their Modeling

In NYISO interconnection planning studies, over a dozen different WTG devices (of WECC Types 1 to 4) have been under consideration. The list of the manufacturers includes, but is not limited to, Acciona, Clipper, Gamesa, GE Energy, Nordex, REpower, Siemens, Suzlon and Vestas. Numerical experiments in this study pertain to a number of these devices.

While most of the considered WTGs are represented by their vendor-specific models (provided by equipment manufacturers), for the other WTGs, models included in the PSS/E Wind Library are applied. With two exceptions, no plant-level control system is represented, which is mainly due to the lack of available simulation tools.

D. Notation for WPPs' Loading Levels

For the sake of simplicity, the loading levels evaluated for WPP-j are defined as $P_j = P_{rj}/n_j$, where n_j = 1, n_j = 2 or n_j = 4. In other words, only active power outputs characterized by the parameter $\lambda_j = P_j/P_{rj} = 1/n_j$ are considered. The rating P_{rj} of WPP-j is calculated as the active power rating of its individual WTG multiplied by the number of WTGs.

Fig. 2 exemplifies the loading levels $\lambda_j = 1$, $\lambda_j = ½$ and $\lambda_j = ¼$ using a typical WTG power curve $P(v_W)$. Here, P is the active power output of an individual WTG under steady state wind speed v_W; v'', v'' and v''' are the cut-in, rated output and cut-out wind speed values, respectively.

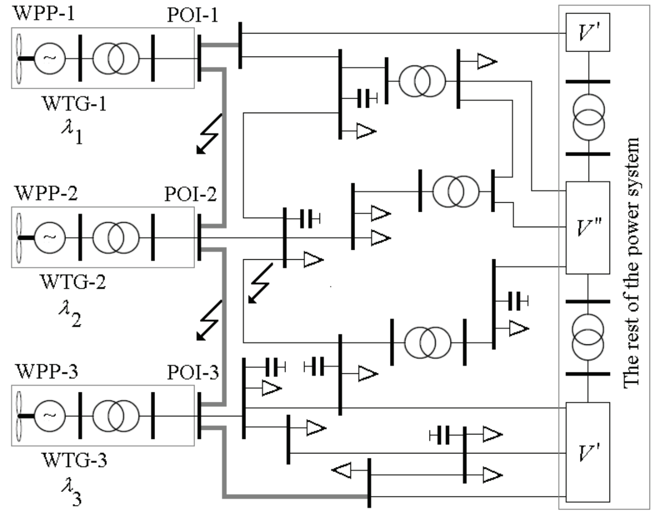

Fig. 1. Schematic diagram of a local area with three WPPs. The bulk power system nominal voltages (like V' and V'') are mostly 115 or 230 kV; elements with lower nominal voltages are assumed but not shown. Danger arrows exemplify fault locations. The circuits depicted in bold grey exemplify transmission lines whose lengths can be varied (see Section III.D).

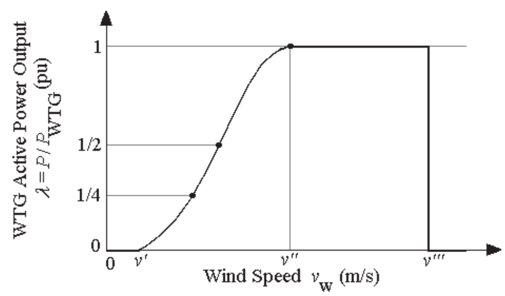

Fig. 2. Loading levels λ shown on a typical WTG power curve.

The partial output with n_j = 2 or n_j = 4 can be achieved in at least two ways: by dispatching all the WTGs of a WPP at the level of $1/n_j$ or leaving online only $1/n_j$ of the WTGs dispatched at full output. For the purpose of this study, only the former situation is of interest.

With regard to the operation at full output (n_j = 1): generally speaking, if the wind speed v_W is between the rated output value v'' and the cut-out value v''', there might be nuances in the WPP dynamic response depending on the exact wind speed. The applied WTG stability models, however, are not expected to be able to reproduce the relevant phenomena.

In terms of PSS/E power flow, the reactive power capability of an equivalent WTG dispatched at the level λ_j is set so that the power factor at the WTG terminals is between +0.95 and -0.95 (except for devices that operate in constant power factor mode).

E. Evaluation Criteria

In the evaluation of contingency simulation results, the following characteristics of the WPP dynamic response are taken into account: major oscillatory modes (their damping and frequency); maximum excursions of variables; the time it takes for transients to decay; and the feasibility of post-contingency steady state. In terms of the FRT capability of a WPP, tripping events are in the focus of attention.

III. Organization of Simulations

For each case study, numerical experiments involve simulations with at least two fault locations and clearing times T_c up to 30 fundamental frequency (60 Hz) cycles.

A. Nearby WPPs' Loading

A combination of the WPPs' loading levels in a local area is characterized by the string vector $[\lambda_1\ \lambda_2\ \lambda_3]$ and hereafter will be referred to by the three-digit number $\Lambda = 100n_1+10n_2+n_3$. As an example, $\Lambda = 124$ means that WPP-1 is at full output and WPP-2 and WPP-3 are loaded at ½ and ¼ of their ratings P_{rj}, respectively. If $\lambda_j = 0$ in the number Λ, the corresponding WPP is offline.

B. Contingencies

Each contingency scenario involves a close-in (to one of the WPPs) three-phase-to-ground fault cleared by tripping a transmission line. A fault is placed either on or near the POI of the WPP or no more than one-two buses from the POI. All faults are applied at time $t = 1$ s. Due to WPP collector losses, the value of P/P_{rj} may slightly differ from λ_j at time $t = 0$ and on the unperturbed simulation interval $\Delta t = [0\ 1)$.

C. Role of Numerical Solution

Some PSS/E WTG models are sensitive to the numerical integration time step size τ [7]. In this study, one of the WPPs tripped with a lesser step τ while it remained online with slightly larger values of τ. For the study experiments, the sensitivity to τ was evaluated to ensure that the τ setting would not lead to ambiguous simulation results.

D. Network Adjustments

To evaluate the impact of electrical distances among the WPPs, the series impedance Z and the charging susceptance B of some transmission lines may be set as $Z = \kappa Z^*$ and $B = \kappa B^*$, where Z^* and B^* refer to actual data and κ is a parameter.

IV. Simulations: Case Studies

This section describes four case studies and provides example simulation plots; a summary of the results is included in Section V. A great deal of data on the NYISO power system and the WPPs fall under the category of CEII. Because of confidentiality concerns, for the considered WTG devices neither the manufacturers nor dynamic models can be specified. Therefore, only general information is provided on the four local areas and the WPPs; the WTGs and their models are referred to by the letters A through E.

A. Case Study CS#1

Here, the three WPPs utilize the same WTG device $\mathrm{WTG_A}$ of Type 3. The POIs are connected as shown in Fig. 1 except for the fact that the WPP-2's POI has no other links to the power system besides the lines to WPP-1 and WPP-3. Figs. 3 and 4 illustrate dynamic responses of WPP-3 and WPP-1.

Because of the two lines connecting POI-2 with POI-1 and POI-3 in this local area, it is interesting to see how the transients are affected by their lengths. For a fault at POI-2, Fig. 4 illustrates the impact of the lines that in Fig. 1 are depicted in bold grey (for $\kappa = 0.5$, $\kappa = 1$ and $\kappa = 2$).

B. Case Study CS#2

Here, the three WPPs utilize different WTG devices: $\mathrm{WTG_B}$ (Type 4) at WPP-1, $\mathrm{WTG_A}$ (Type 3) at WPP-2 and $\mathrm{WTG_C}$ (Type 4) at WPP-3. The number of buses among the three POIs is between 2 and 5. Figs. 5 and 6 illustrate dynamic responses of WPP-1. Note that the WPP-2 transients are very similar to those in case study CS#1 (with $\mathrm{WTG_A}$).

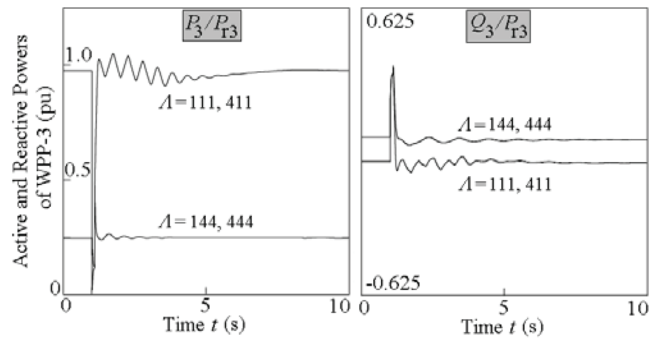

Fig. 3. WPP-3 response to a fault one bus away from POI-1 in CS#1; T_c = 6 cycles; different loading combinations Λ.

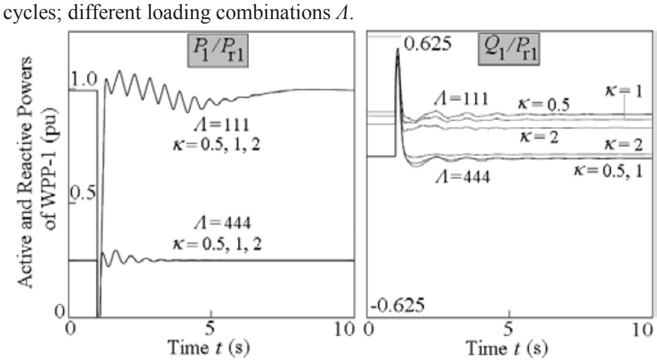

Fig. 4. WPP-1 response to a fault near POI-2 in CS#1; T_c = 6 cycles; different loading combinations Λ and transmission line lengths κ.

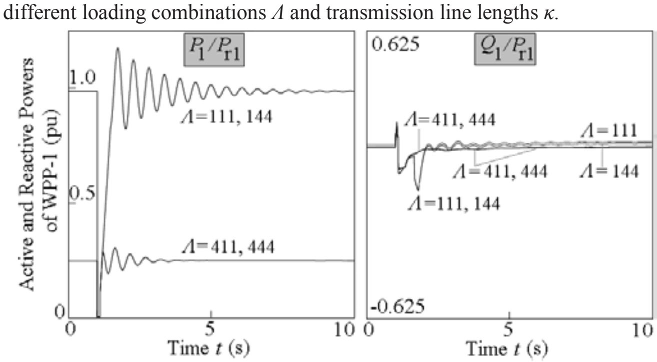

Fig. 5. WPP-1 response to a fault near POI-1 in CS#2; T_c = 6 cycles; different loading combinations Λ.

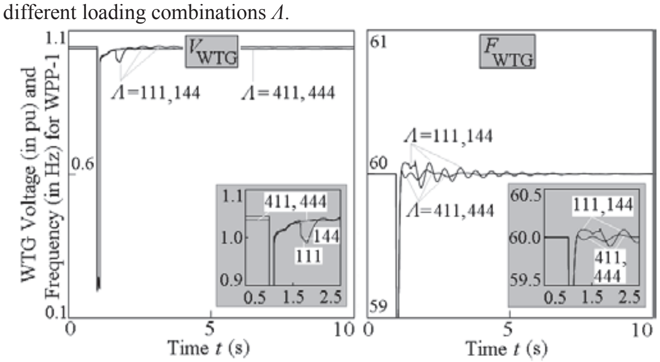

Fig. 6. Response of a WTG at WPP-1 to a fault near POI-1 in CS#2; T_c = 6 cycles; different loading combinations Λ (with zoomed windows).

C. Case Study CS#3

Here, the three WPPs utilize different WTG devices: WTG_C (Type 3) at WPP-1, WTG_D (Type 1) at WPP-2 and WTG_A (Type 3) at WPP-3. WPP-1 and 3 share the same POI, while POI-3 is 5 buses away. Figs. 7 and 8 illustrate dynamic responses of WPP-1 and WPP-3 to a close-in fault near POI-3. For this fault, WPP-3 with loading levels of $\lambda_3 = ½$ and $\lambda_3 = ¼$ trips (at $t = t_{\mathrm{trip}}$) while with full output WPP-3 remains online. Conversely, WPP-1 does not trip.

In Fig. 8 for $\lambda_3 = ½$ and $\lambda_3 = ¼$ (see $\Lambda = 112$ and $\Lambda = 114$), $Q_3 \neq 0$ when $t > t_{\mathrm{trip}}$, which means that the WTG_A model does not zero its reactive power output after tripping. Noteworthy, WPP-3 utilizes the same WTG_A as those at all the WPPs in case study CS#1. Nevertheless, no tripping events are observed in CS#1.

D. Case Study CS#4

Here, the three WPPs utilize the same WTG device WTG_E of Type 3. POI-3 is 4 buses away from POI-1. Figs. 9 and 10 illustrate dynamic responses of WPP-1 and WPP-3. In this case study, WPP-3 with $\lambda_3 = ¼$ (see $\Lambda = 404$) trips for $T_c = 26$ cycles (at $t = t_{\mathrm{trip}}$), unlike the two other WPPs.

Fig. 10 also shows the impact of the lengths of transmission lines in the shortest path between WPP-1 and WPP-3 (for $\kappa = 0.5$ and $\kappa = 1$). With $T_c = 24$ cycles (when no tripping occurs), P_1 noticeably depends on κ for the loading combination $\Lambda = 101$, while for $\Lambda = 404$ the impact is negligible. With $T_c = 26$ cycles (when WPP-3 trips), the impact of κ on P_3 is negligible in any case.

V. SUMMARY OF SIMULATION RESULTS

Rather than analyzing physical mechanisms determining the observed phenomena, including those that lead to tripping events, this study focuses on the end impact of the WPPs' loading. In most numerical experiments (see case studies CS#1 and CS#2), the dynamic response is strongest when a WPP is at full output: the excursions of variables are largest and the time it takes for transients to decay is longest.

Both active power and reactive power responses in most cases show little to no sensitivity to the loading of nearby WPPs. As no POI voltage and frequency plots are included in Section IV, it is worth noting that both variables show almost no sensitivity as well. However, the POI voltage and frequency (immediately after a fault, on the post-fault recovery interval and in the post-contingency steady state) depend considerably on the WPP loading level. With regard to WTG rotor speed curves (not included in Section IV, either): this phenomenon may be noticeably affected by the nearby WTGs' loading even when little impact on other WTG phenomena is observed. Larger rotor speed excursions, however, do not seem to translate into noticeable changes in the electrical phenomena (which might be a modeling issue).

For some of the considered WPPs, the dynamic response, including that in the active power output, may significantly depend on nearby transmission line lengths (more generally, on electrical distances between WPPs). Nevertheless, in most experiments the mutual effect of the loading of nearby WPPs is found negligible as no change in the transients is qualitative.

Conversely, a few numerical experiments (see case studies CS#3 and CS#4) suggest that a WPP at partial load can trip in response to a fault through which it would ride at full output. For a given local area, this effect does not seem to noticeably depend on the nearby WPPs' loading; however, it may depend on electrical distances among WPPs.

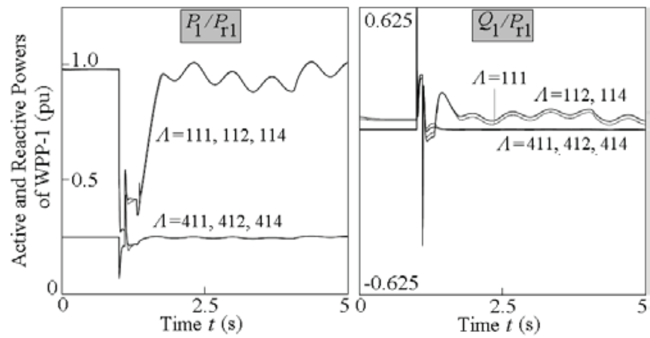

Fig. 7. WPP-1 response to a fault near POI-3 in CS#3; T_c = 6 cycles; different loading combinations Λ.

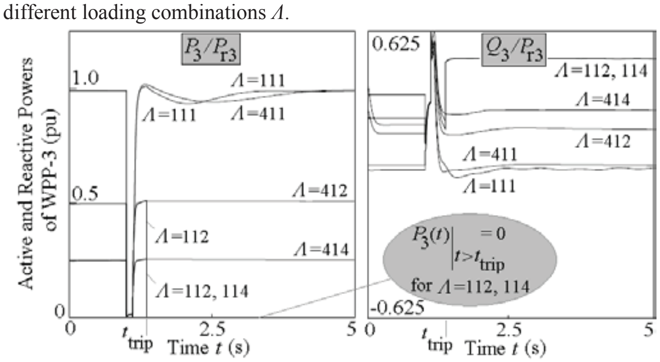

Fig. 8. WPP-3 response to a fault near POI-3 in CS#3; T_c = 6 cycles; different loading combinations Λ.

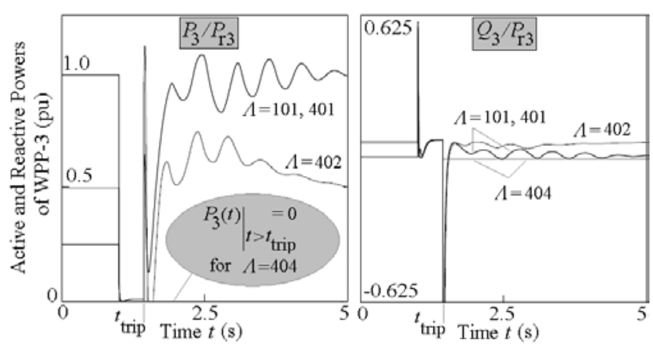

Fig. 9. WPP-3 response to a fault near POI-3 in CS#4; T_c = 26 cycles; different loading combinations Λ.

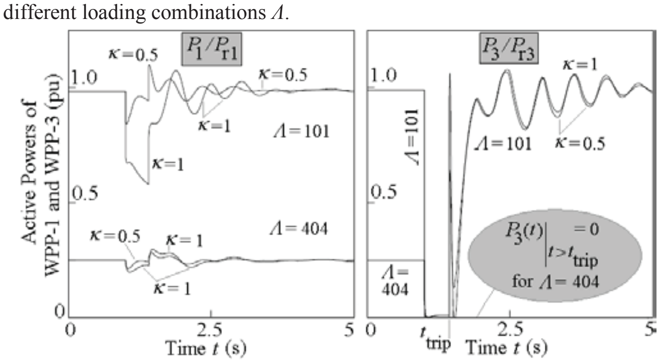

Fig. 10. WPP-1 (left) and WPP-3 (right) responses to faults near POI-3 in CS#4; different loading combinations Λ and transmission line lengths κ. Left: T_c = 24 cycles; right: T_c = 26 cycles.

VI. Discussion

While most numerical experiments confirm the validity of the existing approach to setting the loading level of a WPP, some experiments suggest the opposite. In particular, conclusions on the FRT capability of a WPP can differ depending on its pre-contingency loading. However, similar to [5], [6], this study leaves an impression that its findings are influenced by the specifics of WTG models rather than on the WTG type and device characteristics. Some WTG models are known to have been unable to properly initialize at partial load, not to mention doubts about simulation results. Some current model versions still make it difficult to evaluate WTG behavior under such conditions. While no WTG model with apparent problems of this sort is used in this study, the appropriateness of some applied models is in question.

Currently, many WTG models assume a 2-mass shaft equivalent. In a number of newer models, the turbine aerodynamics module and the shaft system module are significantly reduced or even excluded. An example is the pseudo-governor approach where a simple transfer function mimics the joint action of aerodynamics conversion and blade pitch control [3]. On the other hand, calculations for a Type 3 WTG in [9] suggest that the full mechanical drive train model may exhibit larger excursions in the mechanical torque. If so, even a 2-mass equivalent may lead to a less conservative assessment. While this study has raised concerns about the impact of the nearby WPPs' loading on the rotor speeds, it is unclear whether a WTG model intended for stability studies can reproduce the rotor speed with sufficient accuracy. In addition, for some models, the sufficiency of the module representing the power electronics back-to-back converter (as part of a WTG) may be questioned as well.

Note that in a real large WPP, a variety of factors (including wind speeds, collector configuration, cable types and lengths) are well-known to result in different operating conditions for individual WTGs. Diverse conditions for individual WTGs can make it necessary to represent the collector in more detail [5], [10]. If the WTG rotor speeds and, especially, the diversity of WTG conditions need to be reflected, the effect of WPPs loadings should be reevaluated.

Investigations for a number of the latest WTG models (especially, vendor-specific tools) supplied to the NYISO suggest emerging trends in their evolution toward the use of tools more generic in their nature. Component-based models seem to be giving way to models of rather behavioral type. Noteworthy, for the same WTG device, later model versions often exhibit smoother transients with lesser excursions, especially in the WTG terminal voltage and frequency.

With regard to the latter, more ambiguity arises from analysis of WTG voltage and frequency protection relays data being supplied for some of the newest WPP projects proposed to the NYISO and being customized for these projects by the developers. It is not unusual for the updated relay settings to allow WTGs to remain online for larger and/or longer voltage and frequency excursions. The validity of such updates and their impact on FRT assessment need to be understood better.

VII. Further Work

Both the continued move to behavioral type WTG models and presumable changes in protection relay settings, especially for vendor-specific simulation tools of a more generic nature, should be discussed with WTG manufacturers in more detail.

Usually, the manufacturer of a WTG device develops its EMTP-type model. To understand better the mutual effect of nearby WPPs, a relatively small network area needs to be studied. Simulations based on more accurate EMTP-type tools should be performed to provide more insight into the matter.

VIII. Conclusions

Most numerical experiments have shown that dispatching a WPP at full output leads to the severest stability conditions, while the effect on its dynamic response of the loading of nearby the WPPs is negligible. A few experiments, however, have suggested the opposite. Given that the accuracy of WTG models intended for stability studies may be not sufficient for simulation of partially loaded WTGs, further analysis based on EMPT-type tools is needed. Meanwhile, and especially when a system planning study identifies a concern about the stability of a WPP and/or its FRT capability, more combinations of WPP loading levels should be evaluated.

References

[1] Y. A. Kazachkov, J. W. Feltes and R. Zavadil, "Modeling wind farms for power system studies," in *Proc. of 2003 IEEE PES General Meeting*, July 13-17, 2003, Toronto, Canada.

[2] A. Ellis, Y. Kazachkov, E. Muljadi, J. Sanchez-Gasca, N. Miller, R. Zavadil and P. Pourkeik, "North America Dynamic Wind Generator Modeling Update," IEC TF88 WG27, Oct. 2009, Roskilde, Denmark. Available: http://www.wecc.biz/committees/StandingCommittees/PCC/TSS/MVWG/REMTF/Wind%20Documents/IEC%20TF88-WG27-Oct%202009%20Wind%20Modeling%20Update.pdf

[3] M. Asmine, J. Brochu, J. Fortmann, R. Gagnon, Y. Kazachkov et al., "Model validation for wind turbine generator models," *IEEE Trans. on Power Systems*, Vol. 26, Issue 3, pp. 1769-1782, Aug. 2011.

[4] N. Miller, J. MacDowell, G. Chmiel, R. Konopinski, D. Gautam et al., "Coordinated voltage control for multiple wind plants in Eastern Wyoming: analysis and field experience," in *Proc. of IEEE Power Electronics and Machines in Wind Applications*, July 16-18, 2012, Denver, Colorado, USA.

[5] M. Y. Borodulin, "Effect of wind variation on wind turbine generator dynamics in power system planning stability studies," in *Proc. of 2014 IEEE PES Transmission & Distribution Conference & Exposition*, April 14-17, 2014, Chicago, USA.

[6] M. Y. Borodulin, "Modeling of wind power plant collector system in power system planning stability studies," in *Proc. of 2014 IEEE PES Transmission & Distribution Conference & Exposition*, April 14-17, 2014, Chicago, USA.

[7] M. Y. Borodulin, "Numerical effects in stability simulations of power systems with wind turbine generators," in *Proc. of 2012 IEEE PES General Meeting*, July 22-26, 2012, San Diego, USA.

[8] M. Y. Borodulin, "Validation of wind turbine generator stability models fro wind generation interconnection studies," in *Proc. of 2014 IEEE PES General Meeting*, July 27-31, 2014, Washington DC, USA.

[9] O. Anaya-Lara, G. Ramtharan, E. Bossanyi and N. Jenkins, "Assessment of structural dynamics for model validation of induction generator-based wind turbines," in *Proc. of European Wind Energy Conference*, Feb. 27-March 2, 2006, Athens, Greece

[10] M. A. Elizondo, S. Lu, G. Lin and S. Wang, "Dynamic response of large wind power plant affected by diverse conditions at individual turbines," in *Proc. of 2014 IEEE PES General Meeting*, July 27-31, 2014, Washington DC, USA.